

## Topological phase transitions and holonomies in the dimer model

This article has been downloaded from IOPscience. Please scroll down to see the full text article.

2009 J. Phys. A: Math. Theor. 42 012002

(<http://iopscience.iop.org/1751-8121/42/1/012002>)

View [the table of contents for this issue](#), or go to the [journal homepage](#) for more

Download details:

IP Address: 171.66.16.153

The article was downloaded on 03/06/2010 at 07:30

Please note that [terms and conditions apply](#).

## FAST TRACK COMMUNICATION

# Topological phase transitions and holonomies in the dimer model

Charles Nash<sup>1</sup> and Denjoe O'Connor<sup>2</sup><sup>1</sup> Department of Mathematical Physics, NUIM, Maynooth, Kildare, Republic of Ireland<sup>2</sup> School of Theoretical Physics, DIAS, 10 Burlington Road, Dublin 4, Republic of Ireland

Received 1 October 2008, in final form 24 October 2008

Published 19 November 2008

Online at [stacks.iop.org/JPhysA/42/012002](http://stacks.iop.org/JPhysA/42/012002)**Abstract**

We demonstrate that the classical dimer model defined on a toroidal hexagonal lattice acquires holonomy phases in the thermodynamic limit. When all activities are equal the lattice sizes must be considered mod 6 in which case the finite size corrections to the bulk partition function correspond to a massless Dirac Fermion in the presence of a flat connection with nontrivial holonomy. For general bond activities we find that the phase transition in this model is a topological one, where the torus degenerates and its modular parameter becomes real at the critical temperature. We argue that these features are generic to bipartite dimer models and we present a more general lattice whose continuum partition function is that of a massive Dirac Fermion.

PACS numbers: 05.50.+q, 64.60.Cn, 64.60.-F, 11.25.-w

The classical statistical mechanics of lattice dimer models that interact only via hard-core exclusion are among the simplest exactly solvable two-dimensional models. The subject has a long history and attracted the interest of both mathematicians [1] and physicists [2]. Recently, there have been several surprising advances and these models have re-emerged in new and diverse areas ranging from quantum dimer models [3] to the melting corner/quiver gauge theory circle of ideas in string theory [4]. Furthermore, the dimer model on the hexagonal lattice is closely related to the physics of graphene [5].

Dimer models divide into two classes: those defined on bipartite and non-bipartite lattices—a lattice is bipartite if its sites can be coloured black and white so that adjacent sites are always of the opposite colour. The most general model then assigns a positive number, called an activity, to each bond.

In this communication we focus on the simplest case of *dimers on the hexagonal lattice*, with three distinct activities  $a$ ,  $b$  and  $c$ . We present two principal observations:

- Surprisingly when all activities are set to one the model has a mod 6 structure and the limiting partition function is that of a free massless Dirac Fermion coupled to flat connections.

- As the activities are varied there is a phase transition [2]. We show that at this transition the geometry collapses in a topological phase transition.

The model is critical when none of the activities is larger than the sum of the other two. When considered on a torus, the finite size corrections are that of a free massless Dirac Fermion coupled to a flat connection. The angle between the periods of the torus goes smoothly to zero so that the torus collapses to a degenerate one-dimensional structure at the transition. This geometrical collapse is surprisingly similar to that found recently in a very different context [6].

It has been found [1, 7] that the phase diagram of a bipartite dimer model is described by an *amoeba* obtained from the zero locus of a certain spectral polynomial,  $p(z, w)$ , that arises in the solution of the model on a torus as described below. The amoeba constitutes the parameter domain where the model is critical. In general it has compact and bounding phase boundaries called ovals.

Our results imply that the general situation for bipartite dimer models is therefore as follows: on the amoeba the partition function has finite size corrections corresponding to that of a single massless continuum Dirac Fermion on a torus, coupled to a flat connection. The dimer activities and periodic repetitions of the fundamental cell determine the torus modular parameter and the holonomies of the flat connection. As the boundaries of the compact ovals are crossed there is a phase transition in which the Fermion acquires a Dirac mass [8].

The torus modular parameter,  $\tau$ , gradually changes as one traverses the amoeba until finally as the outer boundary is crossed there is another phase transition where the continuum geometry itself collapses. This transition is continuous—there is no latent heat—but asymmetric. As the transition is approached from the high-temperature side the specific heat diverges with critical exponent  $\alpha = 1/2$ , but there is no divergence as the transition is approached from the low-temperature side.

This transition is very similar to that discussed recently in a three-matrix model [6]. There, as the critical temperature is approached from below, the spherical background geometry evaporates with a diverging specific heat and exponent  $\alpha = 1/2$ , yet there is no divergence if the transition is approached from the high-temperature non-geometrical side.

We begin by constructing the Kasteleyn matrix for the  $N \times M$  covering of a toroidal hexagonal lattice with fundamental tile given in figure 1. We then review the properties of the bulk partition function and discuss the finite size corrections. The communication ends with some speculations on the six-vertex model.

If activities  $a = e^{-\beta\epsilon_a}$ ,  $b = e^{-\beta\epsilon_b}$  and  $c = e^{-\beta\epsilon_c}$  are assigned to the bonds (cf figure 1) then the partition function of the model is given by

$$Z(N, M, a, b, c) = \sum_{\text{coverings}} a^{N_a} b^{N_b} c^{N_c} \quad (1)$$

where  $N_i$  is the number of active bonds of type  $i$  and  $N_a + N_b + N_c = NM$ , since the lattice must be completely covered. When the activities are set to one, equation (1) counts the number of lozenge tilings of the dual triangular lattice.

By assigning signs judiciously to the adjacency matrix, Kasteleyn [9, 10], Fisher and Temperley [11, 12] observed that one can convert (1) into a Pfaffian of, what is now called, a Kasteleyn matrix.

The ‘clockwise odd rule’ [13] is used: arrows are placed on the links in such a way that by assigning +1 when following an arrow and  $-1$  when opposing one, the product of the signs associated with any fundamental plaquette is  $-1$  when the plaquette is circulated in a counter clockwise direction.

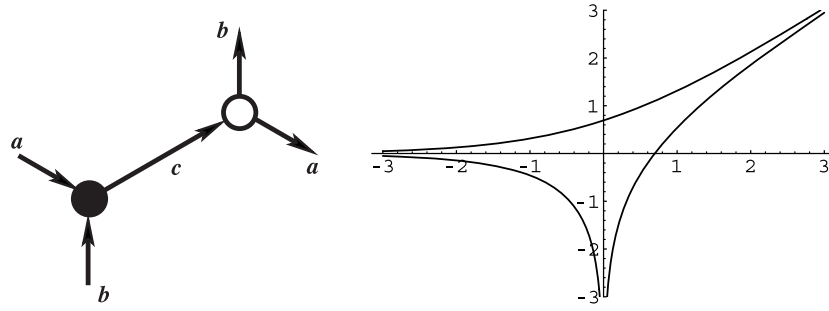


**Figure 1.** The basic tile for the hexagonal lattice, showing the activities and our choice of Kasteleyn orientation and its amoeba.

The Kasteleyn matrix element  $K_{AB}$  is then given by the activity assigned to the link from vertex  $A$  to vertex  $B$  times  $+1$  if the arrow is from  $A$  to  $B$  but times  $-1$  if it is from  $B$  to  $A$ .

A Kasteleyn matrix,  $K$ , is therefore a signed weighted adjacency matrix for the lattice. On any simply connected planar domain, the modulus of the Pfaffian of  $K$  gives the partition function of the dimer model.

On a toroidal lattice the partition function is given by a sum over the different discrete spin structures and therefore involves four terms. This Kasteleyn matrix can in fact be viewed as a lattice Dirac operator [14], or more precisely a lattice version of  $CD$  where  $C$  is the charge conjugation matrix and  $D$  is the Dirac operator. In general a Kasteleyn matrix will describe many lattice Fermions with different masses and the theory of classical dimer models is essentially equivalent to that of two-dimensional lattice Dirac operators.

A consistent sign assignment for the hexagonal lattice is for all arrows to come out of the black vertices and into the white vertices. However, this assignment will not give the standard association of spin structures to the resulting Kasteleyn matrix. So we choose a slightly different convention with  $a$  and  $b$  bonds ingoing to the black vertex and the  $c$  bond outgoing. Then, for this hexagonal lattice, our choice of the Kasteleyn matrix is

$$K = \begin{pmatrix} 0 & A \\ -A^T & 0 \end{pmatrix} \tag{2}$$

where the matrix  $A$  becomes

$$A_{k_1, k_2; l_1, l_2} = c\delta_{k_1, k_2}\delta_{l_1, l_2} - a\delta_{k_1, k_2+1}\delta_{l_1, l_2} - b\delta_{k_1, k_2}\delta_{l_1, l_2+1}. \tag{3}$$

This matrix can be diagonalized using the eigenvectors  $z^k w^{-l}$  and one finds

$$A_{k_1, k_2; l_1, l_2} z^{k_2} w^{-l_2} = (c - a/z - bw) z^{k_1} w^{-l_1} \tag{4}$$

so the eigenvalues are given by the spectral polynomial

$$p^{\text{Hex}}(z, w) = c - a/z - bw. \tag{5}$$

Curiously, this same polynomial also determines the phase diagram in Kitaev’s quantum honeycomb model [15].

For a more complicated tiling (cf figure 2) the analogue of (4) will result in a Fourier transformed Kasteleyn matrix whose off-diagonal block is of size  $d$  where  $d$  is the number of vertices of the same colour in the fundamental domain. The determinant of this matrix will again be a polynomial in  $z$  and  $w$  which will determine the phase diagram for the corresponding bipartite dimer model. On the amoeba of this polynomial  $K$  describes one massless Dirac

Fermion and  $d - 1$  massive ones, with the massive modes decoupling from the problem in the thermodynamic limit.

In the thermodynamic limit the logarithm of the bulk partition function per dimer,  $W = \frac{\ln Z}{NM}$ , is found to be

$$W = \int_0^{2\pi} \frac{d\theta}{2\pi} \int_0^{2\pi} \frac{d\phi}{2\pi} \ln(c - a e^{-i\theta} - b e^{i\phi}). \quad (6)$$

If one of the weights is larger than the sum of the other two, then  $W$  is the logarithm of that weight. There are three such regions, called frozen regions, where one has  $W = \ln a$ ,  $W = \ln b$  and  $W = \ln c$  [10]. The region where none of the weights is larger than the sum of the other two is referred to as the amoeba of the spectral curve  $p^{\text{Hex}}(z, w)$  and is shown in figure 1. On this curve there are exactly two pairs of angles  $(\Theta, \Phi)$  and  $(-\Theta, -\Phi)$  at which  $p^{\text{Hex}} = 0$  where

$$\sin(\Theta) = \frac{b}{2r}, \quad \sin(\Phi) = \frac{a}{2r} \quad \text{and} \quad (7)$$

$$r = \frac{abc}{\sqrt{(a+b+c)(-c+a+b)(c-a+b)(c+a-b)}}. \quad (8)$$

Here,  $r$  is the radius of the circumcircle of the triangle with sides  $a, b$  and  $c$  and opposite angles  $\Phi, \Theta$  and  $\pi - \Theta - \Phi$  respectively. The radius  $r$  diverges, while  $\Theta$  and  $\Phi$  become zero or  $\pi$ , on the boundaries of the amoeba.

A little effort shows that  $W(a, b, c)$  can be expressed in the form

$$W(a, b, c) = \ln c + \frac{\Theta}{\pi} \ln(b/c) + \frac{1}{2\pi i} \left( li_2\left(\frac{a}{c} e^{i\Theta}\right) - li_2\left(\frac{a}{c} e^{-i\Theta}\right) \right) \quad (9)$$

where it was assumed that  $c \geq b \geq a$ . Using the Lobachevsky function<sup>3</sup>

$$L(z) = - \int_0^z \ln|2 \sin(t)| dt, \quad (10)$$

$W$  can be written in the more symmetrical form

$$W(a, b, c) = p_a \ln a + p_b \ln b + p_c \ln c + \text{ent}(a, b, c) \quad (11)$$

where  $\text{ent}(a, b, c)$  is the entropy per dimer and is given by

$$\text{ent}(a, b, c) = \frac{1}{\pi} (L(\pi p_a) + L(\pi p_b) + L(\pi p_c)) \quad (12)$$

with  $p_a + p_b + p_c = 1$  and  $p_a = \Phi/\pi$  and  $p_b = \Theta/\pi$ .

The quantities  $p_a, p_b$  and  $p_c$  are the probabilities that the bonds with activity  $a, b$  and  $c$  respectively, belong to a randomly chosen dimer configuration [17].

As the edge of the amoeba associated with say,  $c$ , is approached  $p_c \rightarrow 1$ . Curiously  $\text{ent}(a, b, c)$  is the Bloch–Wigner dilogarithm  $D(z)$  where  $z$  can be chosen to be the ratio of any two activities (such that  $|z| \leq 1$ ) times the exponential of  $i$  times the angle between them. This latter quantity has  $K$ -theoretic significance [18].

The internal energy  $U = -\frac{\partial W}{\partial \beta}$  is continuous throughout the phase diagram (see [17]) while the specific heat  $C = \beta^2 \frac{\partial^2 W}{\partial \beta^2}$  diverges at the transition [2].

Explicitly, for  $a = b = e^{-\beta}$  and  $c = 1$ , for  $\beta > \ln 2$  we have  $W = U = C = 0$ , and for  $\beta \leq \ln 2$  we have

<sup>3</sup>  $L(z) = \frac{1}{2} Cl_2(2z)$ , where  $Cl_2(x)$  is Clausen's function.

$$W = \frac{2}{\pi} \int_{\beta}^{\ln 2} \cos^{-1} \left( \frac{e^y}{2} \right) dy, \tag{13}$$

$$U = \frac{2}{\pi} \cos^{-1} \left( \frac{e^{\beta}}{2} \right) \quad \text{and} \quad C = \frac{\beta^2}{\pi} \frac{e^{\beta}}{\sqrt{1 - \frac{e^{2\beta}}{4}}}. \tag{14}$$

Expanding around  $\beta_c = \ln 2$ , with  $\ln 2 - \beta \geq 0$  we have

$$W(\beta) \simeq \frac{4\sqrt{2}}{3\pi} (\ln 2 - \beta)^{\frac{3}{2}}. \tag{15}$$

In sum: the transition is continuous with no latent heat. The specific heat is zero in the low-temperature frozen phase; there is a phase transition at  $\beta = \ln 2$ , and the specific heat diverges with critical exponent  $\alpha = \frac{1}{2}$  as the transition is approached from the high-temperature side.

On the torus corresponding to the  $N \times M$  covering by the fundamental tile the partition function is given by

$$\begin{aligned} Z &= (-)^{NM(NM-1)/2} \frac{1}{2} \sum_{u,v=0}^{1/2} e^{2\pi i(\frac{1}{2}+u+v+2uv)} \text{Pfaff} K_{u,v} \\ &= \frac{1}{2} \sum_{u,v=0}^{1/2} e^{2\pi i(\frac{1}{2}+u+v+2uv)} \text{Det} A_{u,v} \end{aligned} \tag{16}$$

with the four terms corresponding to the four discrete spin structures on the torus. For the tiling in figure 1

$$\begin{aligned} \text{Det} A_{u,v} &= \prod_{n=0}^{N-1} \prod_{m=0}^{M-1} p^{\text{Hex}} \left( e^{-\frac{2\pi i(n+u)}{N}}, e^{\frac{2\pi i(m+v)}{M}} \right) \\ &= \prod_{m=0}^{M-1} \left( (c - b e^{\frac{2\pi i(m+v)}{M}})^N - a^N e^{2\pi i u} \right). \end{aligned} \tag{17}$$

The polynomial  $p^{\text{Hex}}$  has two zeros: one at  $z = e^{i\Theta}$ ,  $w = e^{i\Phi}$  the other at  $z = e^{-i\Theta}$ ,  $w = e^{-i\Phi}$ .

Consider, for simplicity, the case when the weights  $a$ ,  $b$ , and  $c$  are such that the angles  $\Theta$  and  $\Phi$  are rational multiples of  $2\pi$ , and in particular such that  $\Theta = -\frac{2\pi n_0}{N}$  and  $\Phi = \frac{2\pi m_0}{M}$ , for integral  $n_0$  and  $m_0$ . Then shifting  $n$  and  $m$  appropriately and expanding around zero at  $(\Theta, \Phi)$  we have

$$p^{\text{Hex}} \simeq -\frac{2\pi i a}{N} e^{-i\Theta} (n + u + \tau(m + v)) \tag{18}$$

where

$$\tau = \frac{Nb}{Ma} e^{i(\Theta+\Phi)}. \tag{19}$$

In the scaling limit,  $N, M \rightarrow \infty$ , with the activities and  $\xi = \frac{N}{M}$  held fixed,  $\tau$  remains constant and becomes the modular parameter of the continuum limit torus. The second zero at  $(-\Theta, -\Phi)$  simply changes  $\tau$  to  $\bar{\tau}$ .

Then for large  $M$  and  $N$  we have

$$\begin{aligned} \lim_{N,M \rightarrow \infty} \frac{Z(N, M)}{e^{NMW(a,b,c)}} &= Z_{\text{Dirac}}(\tau, \theta, \phi) \\ &= \frac{1}{2} \sum_{u,v=0}^{1/2} \left| \frac{\theta[\frac{\theta+u}{\phi+v}](0|\tau)}{\eta(\tau)} \right| \end{aligned} \tag{20}$$

where  $Z_{\text{Dirac}}(\tau, \theta, \phi)$  is the partition function for a Dirac Fermion propagating on the continuum torus with modular parameter  $\tau$  in the presence of a gauge potential with zero field strength, i.e. a flat connection, but with holonomies  $e^{2\pi i\theta}$  and  $e^{2\pi i\phi}$  round the cycles of the torus.

The two zeros of  $p^{\text{Hex}}(z, w)$  guarantee that we are dealing with a continuum limit for a Dirac Fermion, and in the current tiling the Fermion doubling phenomenon is minimized since there are only two vertices in the fundamental tile. A rectangular toroidal domain arises when  $c^2 = a^2 + b^2$  which corresponds to  $\tau_0 = 0$  and  $\tau_1 = \xi \frac{b}{a}$ .

For infinite temperature, where  $a = b = c = 1$  one can see that, if  $N$  and  $M$  are positive integral multiples of 6 then  $\text{Det}A_{0,0} = 0$  in (17) but nonzero otherwise. A similar structure can be seen for other values of  $u$  and  $v$ . A careful study of the limiting form of (17) therefore requires that the limit be taken with the mod 6 periodicity in  $N$  and  $M$  made explicit. Setting  $N = p \bmod 6$  and  $M = q \bmod 6$  we obtain (20) with the modular parameter  $\tau = \xi e^{\frac{2\pi i}{3}}$ ,  $\theta = \frac{1}{2} - \frac{q}{6}$  and  $\phi = \frac{1}{2} + \frac{p}{6}$ .

As the temperature is decreased the angle between the periods of the torus, given by the phase of  $\tau$ , reduces continuously reaching zero when the boundary of the amoeba is reached. For the special case  $a/c = b/c = e^\beta$  the modular parameter takes the form

$$\tau \sim \xi(1 - 4(\ln 2 - \beta) + i2\sqrt{2}\sqrt{\ln 2 - \beta}) + \dots \quad (21)$$

We see that, at the critical temperature  $\beta_c = \ln 2$ , where  $\tau_1 = 0$  while  $\tau_0 = \xi$ , the torus degenerates. It effectively reduces to a line. This is a singular limit of the geometry and is quite distinct from the cylinder limit where for a torus with fixed angle both  $\tau_0$  and  $\tau_1$  go to zero. This phenomenon, of *a singular limit as the boundary of the amoeba is approached* is generic.

Note: for  $\beta = \frac{\ln 3}{2}$  we have  $\tau\left(\frac{\ln 3}{2}\right) = \frac{1}{2} + i\frac{\sqrt{3}}{2} = -\frac{1}{\tau(0)}$ . With zero holonomies, the finite size corrections are modular invariant, and so unchanged under the replacement  $\tau \rightarrow -\frac{1}{\tau}$ , however, the bulk term is different at these two temperatures.

Note also that special care is again needed for  $\Theta$  and  $\Phi$  rational multiples of  $2\pi$ . e.g. when  $a = b$  and  $\Theta = \frac{2\pi p}{q}$ , with  $p$  and  $q$  relatively prime, so that  $\beta = \ln(2 \cos(\Theta))$ , then the lattice sizes  $M$  and  $N$  must be considered modulo  $q$  and one encounters a rich structure of flat connections contributing to the finite size corrections.

The dimer model is also closely related to the six-vertex model and in fact on the free-Fermion line the six-vertex model reduces to a dimer model. In the disordered phase the zero field six-vertex model is critical [19]. As the parameters of the six-vertex model change there is a phase transition, which generically has a latent heat, to a ferroelectric frozen phase [20]. But when the phase boundary is crossed from the disordered phase the specific heat diverges, again with exponent  $\alpha = 1/2$ .

We conjecture that, for the six-vertex model on a torus, as the ferroelectric phase is approached from the disordered phase, the modular parameter,  $\tau$ , decreases to a critical but nonzero value,  $\tau_c$ , and a topological transition occurs. The special case of the dimer model is consistent with this and has  $\tau_c = 0$  consistent with the free-Fermion line.

It was found in [21] (see also [22]) that the six-vertex model with domain wall boundary conditions could be rewritten as a matrix model. The spectrum of eigenvalues of this matrix model changes from continuous to discrete as one crosses the critical line between the disordered and ferroelectric phases. Though this matrix realization of the six-vertex model has not been extended to toroidal boundary conditions it gives some idea of what is happening at a microscopic level as the transition is crossed.

The situation is again reminiscent of what happens in the fuzzy sphere model [6]. However, the high-temperature phase is geometrical with a continuous spectrum in the six-vertex and dimer models, while the geometrical phase in [6] has a discrete spectrum and occurs at low

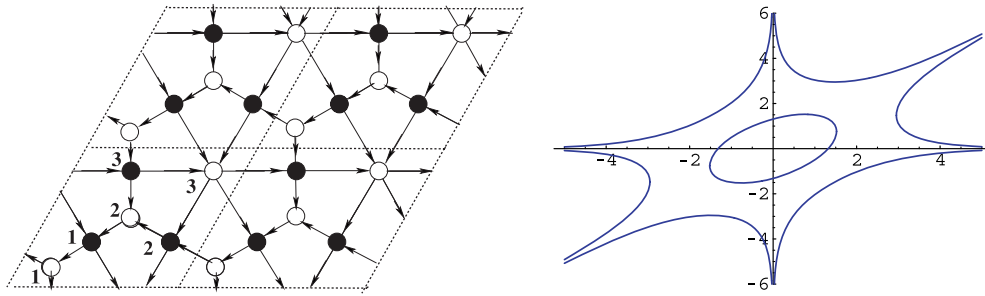


**Figure 2.** Four copies of a Kasteleyn oriented basic tile for the tunable single oval model and its amoeba with  $A_{\pm} = B_{\pm} = C_{\pm} = 1$  and  $D = 10$  in equation (22).

temperatures. The common feature is the asymmetric structure and characteristic divergence of the specific heat in all of these models. We expect that this is generic to such topological transitions.

Finally, we observe that the full generality of features of the bipartite class of dimer models can be accessed in the model whose fundamental tile and amoeba are shown in figure 2. This figure shows a tiling of the torus whose phase diagram or amoeba contains a single compact oval.

The corresponding spectral polynomial is in general

$$p^{\text{Oval}}(z, w) = D - \frac{A_-}{z} - A_+ z - \frac{B_-}{w} - B_+ w - C_- \frac{z}{w} - C_+ \frac{w}{z} \quad (22)$$

where the seven parameters,  $A_{\pm}, B_{\pm}$  etc, are all positive and determined by the 12 link activities and can be parametrized as  $D = 2A \cosh(t_x) + 2B \cosh(t_y) + 2C \cosh(t_{xy})$ ,  $A_{\pm} = Ae^{\pm t_z}$ ,  $B_{\pm} = Be^{\pm t_w}$  and  $C_{\pm} = Ce^{\pm t_c}$ . As the oval is crossed the continuum partition function describes a massive Dirac Fermion and both the Dirac mass and the modular parameter are tunable by adjusting the activities [8].

### Acknowledgments

This work was partly supported by EU-NCG Marie Curie Network No. MTRN-CT-2006-031962.

### References

- [1] Kenyon R, Okounkov A and Sheffield S 2006 *Ann. Math.* **163** 1019–56
- [2] Nagle J F, Yokoi Carlos S O and Bhattacharjee S M 1989 *Phase Transitions and Critical Phenomena* vol 13 ed C Domb and J L Lebowitz (London: Academic) pp 235–97
- [3] Dijkgraaf R, Orlando D and Reffert S 2008 (arXiv:0803.1927)
- [4] Okounkov A, Reshetikhin N and Vafa C 2003 (arXiv:hep-th/0309208)
- [5] Novoselov K S, Geim A K, Morozov S V, Jiang D, Katsnelson M I, Grigorieva I V, Dubonos S V and Firsov A A 2005 *Nature* **438** 197
- [6] Delgadillo-Blando R, O'Connor D and Ydri B 2008 *Phys. Rev. Lett.* **100** 201601
- [7] Kenyon R and Okounkov A 2006 *Duke Math. J.* **131** 499–524
- [8] Nash C and O'Connor D (in preparation)
- [9] Kasteleyn P W 1961 *Physica* **27** 1209–25
- [10] Kasteleyn P W 1963 *J. Math. Phys.* **4** 287–93
- [11] Temperley H N V and Fisher M E 1961 *Phil. Mag.* **6** 1061–3



- [12] Fisher M E 1961 *Phys. Rev.* **124** 1664–72
- [13] Fisher M E 1966 On the Dimer solution of planar Ising models *J. Math. Phys.* **7** 21776–81
- [14] Dijkgraaf R, Orlando D and Reffert S 2007 (arXiv:0705.1645)
- [15] Kitaev A 2006 *Ann. Phys.* **321** 2–111
- [16] Milnor J 1982 *Bull. Am. Math. Soc.* **6** 9–24
- [17] Cohn H, Kenyon R and Propp J 2001 *J. Am. Math. Soc.* **14** 297–346
- [18] Nahm W, Recknagel A and Terhoeven M 1993 *Mod. Phys. Lett. A* **8** 1835
- [19] Baxter R J 1982 *Exactly Solved Models in Statistical Mechanics* (New York: Academic)
- [20] Lieb E H 1967 *Phys. Rev. Lett.* **19** 108
- [21] Zinn-Justin P 2000 *Phys. Rev. E* **62** 3411
- [22] Korepin V and Zinn-Justin P 2000 *J. Phys. A: Math. Gen.* **33** 7053